reduce [NO] and [NO_2] by a decrement y; the corresponding increment to [HNO_2] is neglected, although numerical simulations show that [HNO_2] actually increases by ~10% during the reaction. Reequilibration by K_4 reduces [$IrCl_6^{3-}$] by z (the corresponding decrements to [H^+] and [HNO_2] also being neglected) and increases [NO] and [$IrCl_6^{2-}$] by z. The resulting equilibria are given as

$$K_3 = \frac{([NO]_0 - y + z)([NO_2]_0 - y + x)}{[HNO_2]^2} \quad \text{(A9)}$$

$$K_4 = \frac{([IrCl_6^{3-}]_0 - z)[H^+][HNO_2]}{([IrCl_6^{2-}]_0 + z)([NO]_0 - y + z)} \quad \text{(A10)}$$

Solving eq A10 for y yields

$$y = [NO]_0 - \frac{([IrCl_6^{3-}]_0 - z)[H^+][HNO_2]}{([IrCl_6^{2-}]_0 + z)K_4} + z \quad \text{(A11)}$$

Inserting this expression for y into eq A9 (with the definition $[Ir]_{tot} = [IrCl_6^{2-}]_0 + [IrCl_6^{3-}]_0$) and solving for x yield

$$x = \frac{K_3K_4[HNO_2][IrCl_6^{2-}]}{([Ir]_{tot} - [IrCl_6^{2-}])[H^+]} + [IrCl_6^{2-}] - [NO_2]_0 - \frac{([Ir]_{tot} - [IrCl_6^{2-}])[H^+][HNO_2]}{K_4[IrCl_6^{2-}]} + [NO]_0 - [IrCl_6^{2-}]_0 \quad \text{(A12)}$$

The rate of production of NO_2 through step k_{-2} is defined as

$$dx/dt = 2k_{-2}[NO_3^-][HNO_2][H^+] \quad \text{(A13)}$$

Differentiation of eq A12 and substitution by eq A13 yield the rate law

$$\frac{d[IrCl_6^{2-}]}{dt} = 2k_{-2}[NO_3^-][H^+][HNO_2] \Big/ \left\{1 + [HNO_2] \times [Ir]_{tot}\left(\frac{K_3K_4}{[H^+]([Ir]_{tot} - [IrCl_6^{2-}])^2} + \frac{[H^+]}{k_4[IrCl_6^{2-}]^2}\right)\right\} \quad \text{(A14)}$$

Registry No. $IrCl_6^{3-}$, 14648-50-1; $IrBr_6^{3-}$, 18400-15-2; $[Fe(TMP)_3]^{2+}$, 17378-70-0; HNO_2, 7782-77-6; NO_2, 10102-44-0.

Contribution from the Research Laboratory for Nuclear Reactors, Tokyo Institute of Technology, Meguro-ku, Tokyo 152, Japan, and Department of Chemistry, Miami University, Oxford, Ohio 45056

Kinetics and Mechanism of Ozone Decomposition in Basic Aqueous Solution

HIROSHI TOMIYASU, HIROSHI FUKUTOMI, and GILBERT GORDON*

Received February 1, 1985

The kinetics of the decomposition of ozone have been studied in aqueous alkaline solutions by means of an accumulated stopped-flow method. In slightly basic solution ([OH^-] ~ 0.01 M; 1 M = 1 mol dm^{-3}), the reaction can be described by the following rate law involving first- and second-order terms in ozone: $-d[O_3]/dt = k_1[O_3] + k_2[O_3]^2$. The second-order term is not observed if a radical scavenger (Na_2CO_3) is present in the solution. In solutions of high [OH^-], the rate law changes markedly. The addition of Na_2CO_3 retards the reaction only in the latter stages, and the rate law becomes nearly first order in ozone as the concentration of added Na_2CO_3 is increased. The results provide kinetic evidence for the initiation step $O_3 + OH^- \rightarrow HO_2^- + O_2$, which corresponds to a two-electron-transfer process or an oxygen atom transfer for ozone to hydroxide ion.

Introduction

The current use of ozone in water treatment in the United States and Europe[1-6] has resulted in considerable interest in the chemical reactions and the analytical chemistry of ozone itself.[7-14] The decomposition and redox reactions of aqueous ozone have been reported in detail for more than 50 years. Many facets of the propagation steps in the decomposition of aqueous ozone have been elucidated as a result of a series of cleverly designed kinetic and pulse-radiolysis experiments by Hoigné, Hart, and co-workers.[15-19]

The details of the initiation step in the base-catalyzed decomposition of ozone have been proposed to involve one- and/or two-electron transfer (and/or oxygen atom transfer) involving O_3^-, HO_2^-, O_2^-, and OH as potential intermediates.[2,3,8,15-24]

A variety of early attempts were made to determine the role of ozone, and various orders (and combinations of orders) ranging from 0.5 to 2 have been proposed.[2,3,6,25-39] Unfortunately, many of the studies were not under comparable conditions (i.e. different ozone concentrations, pH, and ionic media, buffers present or absent, possible scavengers and promoters, etc.) resulting in "system-specific" rate constants. The early work of Taube and Bray[35] and others clearly points out the chain-reaction characteristics of the decomposition of aqueous ozone and notes the role of various scavengers such as formic acid, bromide ion, acetic acid, and others. The recent papers by Hoigné, Hart, and co-workers take advantage of scavengers such as acetic acid, carbonate ion, phosphate ion, and *tert*-butyl alcohol in order to define specific systems allowing for the elucidation of the various propagation and termination steps.[10,15-18,40-42]

This paper presents the results of accumulated time-resolved stopped-flow measurements that help to define the role of O_3^-,

* To whom correspondence should be addressed at Miami University.

(1) Symons, J. M. "Ozone, Chlorine Dioxide, and Chloramines as Alternatives to Chorine for Disinfection of Drinking Water"; presented at the Second Conference on Water Chlorination: Environmental Impact and Health Effects, Gatlinburg, TN, Oct 31-Nov 4, 1977.
(2) Peleg, M. *Water Res.* **1976**, *10*, 361.
(3) Zeilig, N. M. *J.—Am. Water Works Assoc.* **1983**, *75*, 34.
(4) Guinvarch, P. *Adv. Chem. Ser.* **1959**, *No. 21*, 416-429.
(5) Katzenelson, E.; Kletter, B.; Shuval, H. I. *J.—Am. Water Works Assoc.* **1974**, *66*, 725-729.
(6) Gorol, M. O.; Singer, P. C. *Environ. Sci. Technol.* **1982**, *16*, 377.
(7) "Standard Methods for the Examination of Water and Wastewater", 14th ed.; American Public Health Association: Washington, DC, 1975.
(8) Gordon, G.; Grunwell, J. "Proceedings of the Second National Symposium on Municipal Waste Water Disinfection"; Venosa, A., Akin, E. W., Eds.; United States Environmental Protection Agency: Cincinnati, OH, 1982; Vol. 18, pp 226-245.
(9) Bader, H.; Hoigné, J. *Ozone: Sci. Eng.* **1982**, *4*, 169.
(10) Hoigné, J.; Bader, H. *Vom Wasser* **1980**, *55*, 261.
(11) Tomiyasu, H.; Gordon, G. *Anal. Chem.* **1984**, *56*, 752.
(12) Straka, M. R.; Pacey, G. E.; Gordon, G. *Anal. Chem.* **1984**, *56*, 1973.
(13) Grunwell, J.; Benga, J.; Cohen, H.; Gordon, G. *Ozone: Sci. Eng.* **1983**, *5*, 203.
(14) Stanley, J.; Johnson, D. "Handbook of Ozone Technology and Applications"; Rice, R. G., Netzer, A., Eds.; Ann Arbor Science (The Butterworth Group): Ann Arbor, MI, 1982; pp 255-276.
(15) Staehelin, J.; Hoigné, J. *Vom Wasser* **1977**, *48*, 283.
(16) Fornl, L.; Bahnemann, D.; Hart, E. J. *J. Phys. Chem.* **1982**, *86*, 255.
(17) Buhler, R. E.; Staehelin, J.; Hoigné, J. *J. Phys. Chem.* **1984**, *,8*, 2560.
(18) Sehested, K.; Holcman, J.; Bjergbakke, E.; Hart, E. J. *J. Phys. Chem.* **1984**, *88*, 269.
(19) Sehested, K.; Holcman, J.; Bjergbakke, E.; Hart, E. J. *J. Phys. Chem.* **1982**, *86*, 2066.
(20) Ivanov, Yu. E.; Nikitina, G. P.; Pushlenkov, M F.; Shunkov, V. G. *Zh. Fiz. Khim.* **1972**, *46*, 2163.

0020-1669/85/1324-2962$01.50/0 © 1985 American Chemical Society

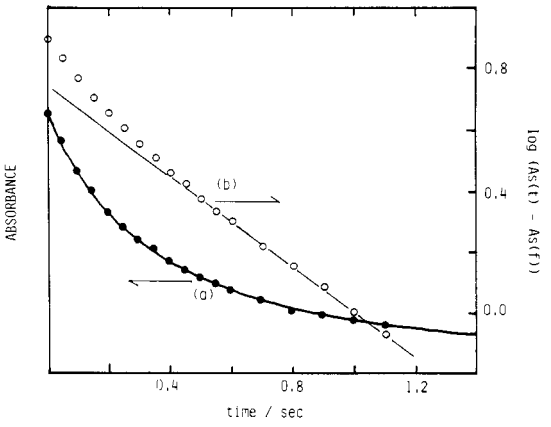

Figure 1. Solid line (a): Accumulated stopped-flow trace at 260 nm obtained in pure alkaline solution under the conditions $[O_3]_0 = 3.16 \times 10^{-5}$ M and $[OH^-] = 0.00717$ M at 20 °C. ○: Plot of log [As(t) − As(f)] vs. time for trace a. ●: Nonlinear least-squares fits to the rate equation, $-d[O_3]/dt = k_1[O_3] + k_2[O_3]^2$, with $k_1 = 1.26$ s^{-1} and $k_2 = 6.4 \times 10^4$ M^{-1} s^{-1}.

HO_2, HO_2^-, O_2^-, and OH as intermediates. Direct evidence is also presented for oxygen transfer from ozone to hydroxide ion to form HO_2^- as the initiation step.

Experimental Section

Ozone was generated by an electric discharge in dry oxygen and dissolved in triply distilled water. Carbonate-free sodium hydroxide, sodium carbonate, and hydrogen peroxide were of reagent grade (Wako Pure Chemical Ind. Ltd.) and were used without further purification. A Union Giken RA 401 stopped-flow instrument was used for the accumulated stopped-flow measurements. In general, a minimum of 10 individual traces were accumulated in order to enhance the signal to noise ratio.

Ozone, sodium hydroxide, and sodium carbonate solutions were introduced into the stopped-flow spectrometer by using gas-tight syringes that acted as storage reservoirs. These syringes were linked directly to the two spectrophotometer drive syringes by means of all-Pyrex connections.

Results

A typical stopped-flow trace for the decomposition of ozone in slightly basic water ($[OH^-] = 7.17 \times 10^{-3}$ M, 1 M = 1 mol/dm^{-3}) and a pseudo-first-order plot (a plot of log [As(t) − As(f)] vs. time) are shown in Figure 1 where As(t) and As(f) refer to the relative absorbances at 260 nm at time = t and infinity, respectively. As can be seen in Figure 1, the plot deviates markedly from a straight line in the initial stages. However, the observed stopped-flow data can be fitted satisfactorily to the values calculated from the following empirical rate equation involving both first- and second-order terms:

$$-d[O_3]/dt = k_1[O_3] + k_2[O_3]^2$$

Under the conditions $[OH^-] = 7.17 \times 10^{-3}$ M and initial ozone concentration $[O_3]_0 = 3.16 \times 10^{-5}$ M, k_1 and k_2 were determined to be 1.26 s^{-1} and 6.4×10^4 M^{-1} s^{-1}, respectively. The values of k_1 and k_2 vary markedly as a function of solution composition.[2,3,6,25-39] In Figures 2 and 3, stopped-flow traces for the decomposition of ozone in slightly basic water involving 0.5×10^{-3} and 3×10^{-3} M Na_2CO_3 and plots of log [As(t) − As(f)] vs. time are shown. In these reactions, the pseudo-first-order plots also deviate from linearity in the initial stages. However, the deviation differs from that in pure water, since the initial rates observed

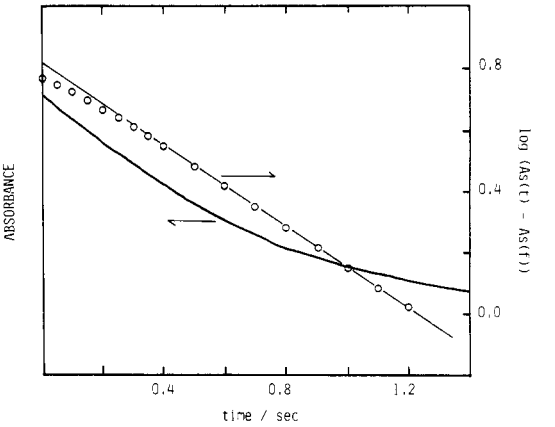

Figure 2. Accumulated stopped-flow trace at 260 nm in a slightly basic solution containing 0.5×10^{-3} M Na_2CO_3. $[O_3] = 2.88 \times 10^{-5}$ M, $[OH^-] = 0.00802$ M at 20 °C. ○: Plot of log [As(t) − As(f)] vs. time.

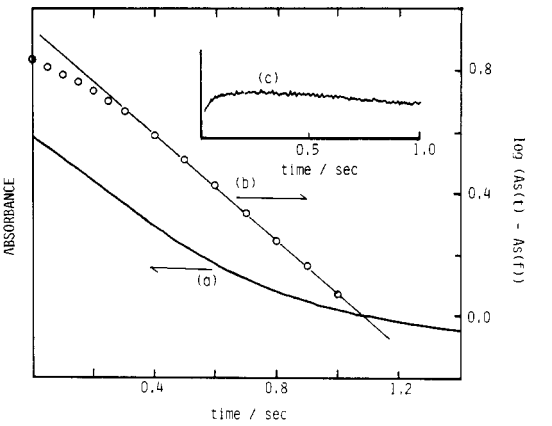

Figure 3. Stopped-flow data at 260 nm in a slightly basic solution containing 3×10^{-3} M Na_2CO_3 under the conditions $[O_3]_0 = 2.88 \times 10^{-5}$ M and $[OH^-] = 0.0117$ M at 20 °C: (a) accumulated trace at 260 nm; (b) plot of log [As(t) − As(f)] vs. time for trace a; (c) accumulated trace at 600 nm, which demonstrates the formation of the carbonate radical.

Table I. Apparent First-Order Rate Constants for the Decomposition of Ozone in the Presence of Sodium Carbonate

$[O_3]_0$, 10^{-5} M	$[OH^-]$, 10^{-3} M	$[Na_2CO_3]$, 10^{-3} M	k_{app},[a] s^{-1}	k_{OH^-},[a] M^{-1} s^{-1}
3.16	7.17	0	1.26[b]	176
2.88	8.02	0.5	1.52	190
2.88	10.3	1.5	1.89	183
2.83	11.0	3.0	1.97	179

[a] k_{ap+} and k_{OH^-} are defined as $-d[O_3]/dt = k_{app}[O_3] = k_{OH^-}[OH^-][O_3]$. [b] The value corresponds to k_1 in the equation $-d[O_3]/dt = k_1[O_3] + k_2[O_3]^2$.

(21) Hoigné, J.; Bader, H. *Chimia* **1975**, *29*, 20.
(22) Stachlin, J. Ph.D. Thesis, ETH-Zurich, 1983.
(23) Gorbenko-Germanov, D. S.; Kozlova, I. V. *Dokl. Akad. Nauk SSSR* **1973**, *210*, 851–854.
(24) Gorbenko-Germanov, D. S.; Kozlova, I. V. *Zh. Fiz. Khim.* **1974**, *48*, 166–168.
(25) Rothmund, V.; Burgstaller, A. *Monatsh. Chem.* **1913**, *34*, 665–692.
(26) Sennewald, K. *Z. Phys. Chem., Abt. A* **1933**, *A164*, 305–317.
(27) Weiss, J. *Trans. Faraday Soc.* **1935**, *31*, 668–681.
(28) Alder, M. G.; Hill, G. R. *J. Am. Chem. Soc.* **1950**, *72*, 1884–1886.
(29) Stumm, W. *Helv. Chim. Acta* **1954**, *37*, 773–778.
(30) Kilpatrick, M. L.; Herrick, C. C.; Kilpatrick, M. *J. Am. Chem. Soc.* **1956**, *78*, 1784–1790.
(31) Rankas, M. M.; Siirode, E. K.; Kyulm, S. R. *Chem. Abstr.* **1964**, *60*, 2633e.
(32) Czapski, G.; Samuni, A.; Yellin, R. *Isr. J. Chem.* **1968**, *6*, 969–971.
(33) Hewes, C. G.; Davison, R. R. *AIChE J.* **1971**, *17*, 1, 141–147.
(34) Merkulova, V. P.; Louchikov, V. S.; Ivanovskii, M. D. *Izv. Vyssh. Uchebn. Zaved., Khim. Khim. Technol.* **1971**, *14*, 5.
(35) Taube, H.; Bray, W. C. *J. Am. Chem. Soc.* **1940**, *62*, 3357.
(36) Roth, J. S.; Sullivan, D. E.; D'Ambrosi, M. "Ozonews Technical Paper Section"; International Ozone Association: Vienna, VA, 1979; Vol. 7.
(37) Gilbert, E. *Vom Wasser* **1974**, *43*, 275.
(38) Gilbert, E. *Water Res.* **1980**, *14*, 1637.
(39) Joy, P.; Gilbert, E.; Eberle, S. H. *Water Res.* **1980**, *14*, 1509.
(40) Hoigné, J.; Bader, H. In "Organometals and Organometalloids; Occurrence and Fate in the Environment"; Brinkmann, F. E., Bellama, J. M., Eds.; American Chemical Society: Washington, DC, 1978; ACS Symp. Ser. No. 82, p 292.
(41) Hoigné, J.; Bader, H. *Water Res.* **1976**, *10*, 377.
(42) Staehlin, J.; Hoigné, J. *Vom Wasser* **1983**, *55*, 337.

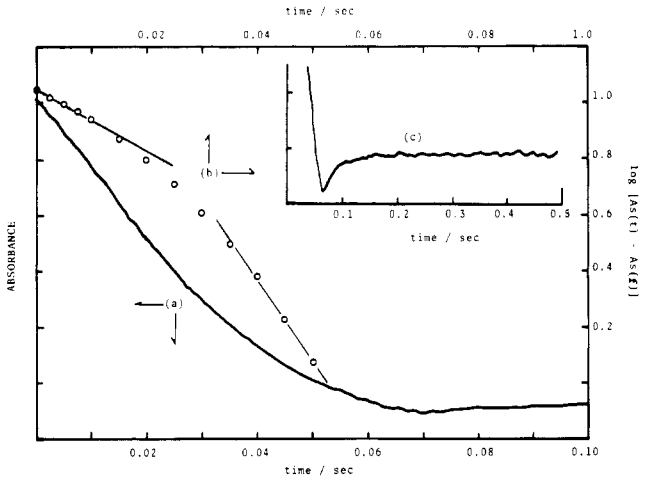

Figure 4. (a, c) Accumulated stopped-flow traces at 260 nm in pure alkaline solution under the conditions $[O_3]_0 = 4.92 \times 10^{-5}$ M and $[OH^-] = 0.117$ M at 20 °C. (b) Plot of log [As(t) − As(f)] vs. time for trace a.

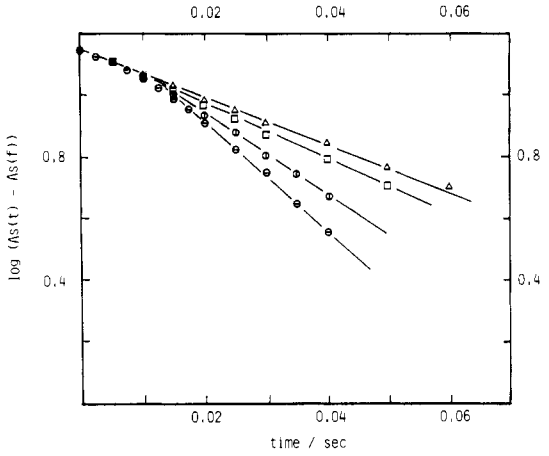

Figure 5. Plots of log [As(t) − As(f)] vs. time for the accumulated stopped-flow data obtained at 260 nm in alkaline solutions containing various concentrations of Na_2CO_3 at 20 °C, $[O_3]_0 = 3.03 \times 10^{-5}$ M, and $[OH^-] = 0.126$ M. [Na_2CO_3], M: ⊖, 0; ⊕, 0.5×10^{-3}; □, 1.5×10^{-3}; △, 3×10^{-3}.

in the presence of Na_2CO_3 are slower than those of the following latter part of reactions. Such a deviation increases as the concentration of Na_2CO_3 increases.

In Figure 3, a stopped-flow trace measured at 600 nm is also shown. According to the earlier work by Hart[16,19] and Hoigné,[9,10,15,17] the trace reveals the formation of the carbonate radical, CO_3^-. It should be noted that the carbonate radical is accumulated within 300 ms after the mixing of ozone with alkali solutions involving Na_2CO_3 and that the time scale is well correlated to the deviation from linearity in plot b in Figure 3. The apparent first-order rate constants, k_{app}, which were obtained in the presence of Na_2CO_3 from the linear plot of the pseudo-first-order plots such as are shown in Figures 2 and 3, are listed in Table I together with the second order-rate constant, k_{OH^-}, which is defined as $k_{app} = k_{OH^-}[OH^-]$. The average value for k_{OH^-} for the latter portion of the reaction is 182 ± 4 M^{-1} s^{-1}. The value of k_{OH^-} was also determined from the initial stage in Figure 3 to be 111 M^{-1} s^{-1}.

The rate of ozone decomposition and the shape of the pseudo-first-order plots in pure alkaline solutions change markedly with the concentration of OH^-. In the solutions of high OH^- concentrations ($[OH^-] \approx 0.1$ M), a plot of log [As(t) − As(f)] vs. time shows marked deviations from linearity (Figure 4). However, the tendency of the deviation is completely different from that shown in Figure 1, because in high OH^- solutions the initial rate is slower than the rate for the latter part of the reaction. The addition of Na_2CO_3 also gives different effects on the rates.

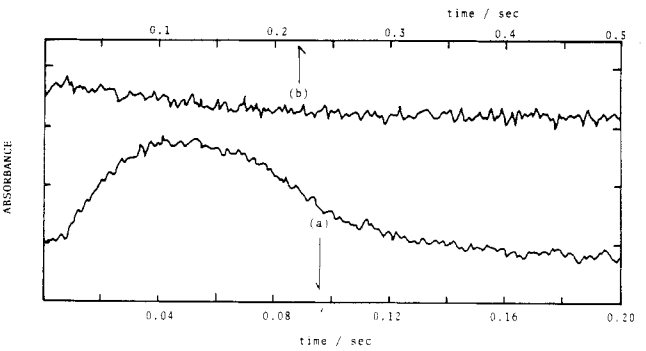

Figure 6. Accumulated stopped-flow traces at 430 nm in the alkaline solution under the conditions $[O_3]_0 = 4.92 \times 10^{-5}$ M and $[OH^-] = 0.117$ M at 20 °C: (a) trace obtained in the pure alkaline solution; (b) trace obtained in the same alkaline solution containing approximately 0.01 M Na_2CO_3.

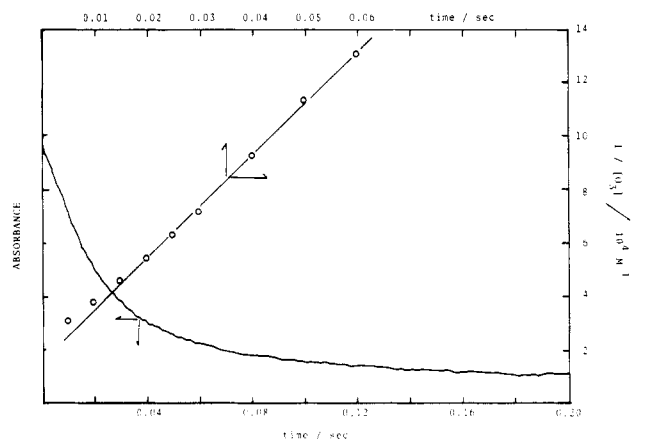

Figure 7. Typical accumulated stopped-flow trace at 260 nm after the rapid mixing of O_3 with H_2O_2 under the conditions $[O_3]_0 = 4.23 \times 10^{-5}$ M, $[H_2O_2] = 3.0 \times 10^{-5}$ M, and $[OH^-] = 7.27 \times 10^{-3}$ M at 20 °C. ○: Plot of $1/[O_3]$ vs. time.

As can be seen in Figure 5, the initial rates are changed only slightly by the addition of Na_2CO_3, while the latter parts are retarded depending on the concentration of added Na_2CO_3.

The ozone decomposition was complete within 0.07 s in pure alkaline solution ($[OH^-] = 0.117$ M) as can be seen in Figure 4. However, after completion of the ozone decomposition, the absorbances at 260 nm increased (insert of Figure 4). According to earlier reports,[16,19] this is indicative of the formation of superoxide ion O_2^-.

In Figure 6, stopped-flow traces at 430 nm in alkaline solution ($[OH^-] = 0.117$ M) are shown, where the change in the absorbance has a maximum at 40–50 ms (Figure 6a). We interpret the stopped-flow trace as revealing[19] the appearance of ozonide ion O_3^-. Ozonide ion was also formed in the solution containing 0.01 M Na_2CO_3, but the amount was considerably less than that formed in the pure alkaline solution (see Figure 6b).

The reaction between O_3 and H_2O_2 was also measured by the stopped-flow method. In Figure 7, a typical stopped-flow trace and a plot of $1/[O_3]$ vs. time are shown. The linearity of the plot except for the initial stage (i.e. a short induction period) indicates that the reaction can be treated as a first-order process for both ozone and H_2O_2 such that

$$O_3 + HO_2^- \xrightarrow{k_{HO_2^-}} \text{products}$$

where

$$H_2O_2 \rightleftharpoons H^+ + HO_2^- \quad pK = 11.65$$

The apparent second-order rate constant for the linear portion of the reaction as shown in Figure 7 was determined to be 1.94×10^6 M^{-1} s^{-1}. From the value of $pK_{H_2O_2} = 11.65$, $k_{HO_2^-}$ was calculated to be 3.1×10^6 M^{-1} s^{-1}. In view of the markedly

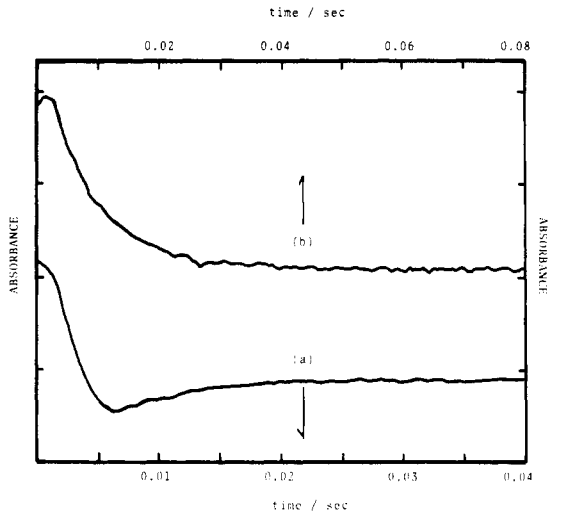

Figure 8. Accumulated stopped-flow traces after rapid mixing of O_3 with H_2O_2 under the conditions $[O_3]_0 = 4.92 \times 10^{-5}$ M, $[H_2O_2]_0 = 2.5 \times 10^{-4}$ M, and $[OH^-] = 0.117$ M at 20 °C: (a) trace at 260 nm (O_3 disappearance, O_2^- appearance); (b) trace at 430 nm (O_3^- appearance).

different experimental conditions, this value agrees satisfactorily with the value of 5.5×10^6 M^{-1} s^{-1} by Hoigné[15] at pH 6. Plots of the kinetic data for the reaction between O_3 and H_2O_2 in highly basic solutions (0.117 M OH^-) are also shown in Figure 8. The rate of ozone decomposition was too fast to be measured with our apparatus ($t_{1/2} << 1$ ms), but the appearance of O_2^- was monitored at 260 nm and the rapid formation and subsequent decomposition of O_3^- was recorded after the initial induction period.

Discussion

It seems to be most probable on the basis of the earlier work[9,10,15-19] that the decomposition of ozone in basic solution is initiated by means of one or more of the three reactions[9,17,19,22,24,27]

$$O_3 + OH^- \rightarrow O_3^- + OH \quad (1)$$

$$O_3 + OH^- \rightarrow HO_2^- + O_2 \quad (2)$$

$$O_3 + OH^- \rightarrow O_2^- + HO_2 \quad (3)$$

where HO_2 would be in rapid equilibrium with O_2^-:

$$HO_2 \rightleftharpoons H^+ + O_2^- \quad pK = 4.8$$

Reactions 1 and 2 are clearly thermodynamically favorable. Reaction 1 corresponds to a direct one-electron-transfer process whereas reaction 2 corresponds to a two-electron-transfer or an oxygen atom transfer reaction. On the other hand, reaction 3 formally corresponds to an oxygen radical (O^+) transfer or to an oxygen atom transfer from ozone to hydroxide ion concomitant with an electron transfer from hydroxide ion to ozone. On this basis, reaction 3 would appear to be the least probable process.

In a series of continuing reactions, peroxide anion (HO_2^-) and superoxide anion (O_2^-) react further with ozone to form ozonide ion (O_3^-):

$$HO_2^- + O_3 \rightarrow O_3^- + HO_2$$

$$HO_2 + OH^- \rightarrow O_2^- + H_2O \quad \text{(very rapid)}$$

$$\text{net: } HO_2^- + O_3 \xrightarrow{OH^-} O_3^- + O_2^- + H_2O \quad (4)$$

and[16,19]

$$O_2^- + O_3 \rightarrow O_3^- + O_2 \quad 1.6 \times 10^9 \text{ } M^{-1} \text{ } s^{-1} \quad (5)$$

Furthermore, ozonide ion (O_3^-) ultimately decomposes to form OH radicals[17,19] by means of the reactions

$$O_3^- + H^+ \rightarrow HO_3 \quad 5 \times 10^{10} \text{ } M^{-1} \text{ } s^{-1} \quad (6)$$

$$HO_3 \rightarrow OH + O_2 \quad 1.4 \times 10^5 \text{ } s^{-1} \quad (7)$$

or by

$$O_3^- \rightarrow O^- + O_2 \quad (8)$$

$$O^- + H_2O \rightarrow OH + OH^- \quad (9)$$

Finally the OH radical can additionally react with more ozone to form more superoxide anion (O_2^-) directly

$$OH + O_3 \rightarrow HO_2 \text{ (or } O_2^- + H^+) + O_2 \quad (10)$$

$$\text{(or)} \quad O^- + O_3 \rightarrow O_2^- + O_2$$

which in turn initiates a chain reaction (5) followed by reactions 6 and 7.

Hoigné has suggested reaction 10 mechanistically involves the formation of HO_4

$$OH + O_3 \rightarrow [O_3 \cdot OH] \quad 3 \times 10^9 \text{ } M^{-1} \text{ } s^{-1} \quad (11)$$

followed by

$$[O_3 \cdot OH] \rightarrow HO_2 + O_2 \quad 3 \times 10^4 \text{ } s^{-1} \quad (12)$$

$$[O_3 \cdot OH] \rightarrow O_3 + O_2 + H_2O \quad <10^{10} \text{ } s^{-1} \quad (13)$$

If Na_2CO_3 is added to ozone solutions of low OH^- concentrations ($[OH^-] = 0.01$ M), the decomposition rates are retarded especially at the initial stage as shown in Figures 2 and 3. This indicates that the second-order term of the rate law for ozone decomposition in the pure alkaline solution should be attributed to the chain-reaction process that is initiated from the reaction with the OH radical, since only OH radicals are scavenged[15] by Na_2CO_3. Using Na_2CO_3 as a scavenger, Hoigné et al.[15] determined the stoichiometric yield of OH radicals during the decomposition of ozone to be 0.55 ± 0.08. This was much less than the value of 2 that was expected on the assumption that eq 1 represented the initiation process. On the other hand, the stoichiometric yield was consistent with reactions 2 and 3 for the initiation process. As will be described later, our data support this conclusion.

The rate of ozone decomposition which is initiated by means of the OH radical can be expressed by

$$\text{rate (chain)} = k_{11}[O_3][OH] \quad (14)$$

Since the rates of reaction 5 and the decomposition of O_3^- are found to be much faster than that of the initiation reaction 2 or 3 (compare Figures 1–3 with Figures 6 and 7) in the solutions of such low $[OH^-]$, the concentration of OH radical is proportional to that of O_3 and OH^-. Thus

$$[OH]_{ss} = \frac{2k_{OH^-}[O_3][OH^-]}{k_s[S]} \quad (15)$$

where $k_s[OH][S]$ is the rate for scavenging of OH radicals by other radicals or by impurities that might be present in the solution. The inclusion of eq 10 and 11 results in a second-order term for ozone in the overall rate equation (16). Hart et al.[16] suggest that

$$-\frac{d[O_3]}{dt} = k_{OH^-}[OH^-][O_3] + \frac{2k_{OH^-}[OH^-][O_3]^2}{k_s[S]} \quad (16)$$

the carbonate radical (CO_3^-) that is accumulated at the initial stages of the reaction and then decreases (insert of Figure 3), reacts with ozone, and hence only the initial rate provides the real value for k_{OH^-}. The value of k_{OH^-} obtained from the initial stage shown in Figure 3 is 111 M^{-1} s^{-1}. This value agrees very well with that of 109 ± 43 M^{-1} s^{-1} obtained by Hart.[16] In Figure 3, the latter part of ozone decomposition gives $k_{OH^-} = 182$ M^{-1} s^{-1}, which is 64% larger than the value from the initial stage. The larger value of the latter part may be attributed to an additional reaction between CO_3^- and ozone:

$$CO_3^- + O_3 \rightarrow \text{products } (CO_2 + O_2^- + O_2) \quad (17)$$

On the assumption that ozone decomposition is initiated by means of reaction 2 (or (3)) followed by reactions 4–9, three ozone molecules produce two OH radicals and hence produce two CO_3^- radicals. If each CO_3^- radical reacts with one ozone molecule, the rate of ozone decomposition in the presence of Na_2CO_3 should

Table II. Apparent First-Order Rate Constants for the Decomposition of O_3^- in the Presence and the Absence of Sodium Carbonate at 20 °C

$[O_3]$, 10^{-5} M	$[OH^-]$, M	$[Na_2CO_3]$, 10^{-4} M	$k_{O_3^-}$,[a] s^{-1}
1.42	0.0649		17 ± 6
2.30	0.0947		15 ± 6
2.30	0.0968	5	13 ± 6
4.92	0.117		30 ± 3

[a] $-d[O_3^-]/dt = k_{O_3^-}[O_3^-]$.

be about 66% larger in the latter part of the reaction as compared to the rate of the initial stage of the reaction. At the same time the products in reaction 17 would not participate in any additional reactions with ozone.

It should also be noted that in slightly basic ozone solutions (pH 8–10) where the rate of initiation reaction $k_{OH^-}[OH^-][O_3]$ is much slower than that of the reaction between O_3 and the CO_3^- radical, ozone decoposition would proceed via a simple pseudo-first-order reaction over the whole time scale. Hoigné et al.[15] demonstrated the linearity of a plot of log $([O_3]/[O_3]_0)$, (where $[O_3]_0$ denoted the initial concentration of ozone) vs. time in the presence of Na_2CO_3 at pH = 10.

As the concentration of OH^- increases, pseudo-first-order plots for the ozone decomposition in pure alkaline solution change markedly. The addition of Na_2CO_3 in the strongly basic solutions also reveals a drastic change as noted in Figure 5, where the retardation effect by Na_2CO_3 is observed markedly in the latter parts of the reaction. This fact that the initial rate is not affected by added Na_2CO_3 rules out the possibility of reaction 1 for the initiation of ozone decomposition, because the OH radical is generated directly in reaction 1. In the presence of 3×10^{-3} M Na_2CO_3, the pseudo-first-order plots become linear, giving $k_{OH^-} = 130\ M^{-1}\ s^{-1}$.

The critical point to determine the shape of pseudo-first-order plots for ozone decomposition at various OH^- concentrations could be attributed to the difference in the rates of initiation, $k_{OH^-}[OH^-][O_3]$, and of decomposition of O_3^-. From Figure 6 the observed first-order rate constant for the decomposition of O_3^- is calculated roughly to be 20–30 s^{-1}. Additional experiments in slightly less basic solutions are shown in Table II.

This indicates that the rate of O_3^- decomposition is much faster than that of the decomposition of ozone under mildly basic conditions such as are shown in Figures 1–3. Therefore, under such conditions, the chain reaction that is accompanied by the decomposition of O_3^- takes place simultaneously after reaction 2 or 3, and hence eq 16 can be applied directly.

On the other hand, in strongly basic solutions ($[OH^-] \approx 0.1$ M), the chain reaction occurs after an interval of about 0.02 s, during which O_3^- is accumulated. In this case the chain reaction does not give the second-order term for the ozone decomposition, since the concentration of O_3^- is no longer proportional to that of ozone. Therefore, the addition of Na_2CO_3 retards the ozone decomposition in only the latter part of the reaction, and the pseudo-first-order plots are nearly linear as the added Na_2CO_3 increases, because the CO_3^- radical that results from the scavenging of the OH radical does not react with ozone on this time scale.

Although it has been possible to rule out the direct-electron-transfer reaction from OH^- to O_3 (eq 1), it is not possible from kinetic experiments alone to determine whether reaction 2 or 3 initiates the ozone decomposition process. If reaction 3 is assumed for the initiation, O_3^- should be accumulated simultaneous with the decomposition of ozone at the initial stage of the reaction, since reaction 5 is known[17] to be extremely fast ($k_5 = 1.5 \times 10^9\ M^{-1}\ s^{-1}$). As can be seen in Figure 6, there is an induction period for the accumulation of O_3^-. If reaction 2 is assumed as the initiation step, the accumulation of O_3^- would be delayed, since reaction 4 is not instantaneous (see Figure 7) when compared with reaction 2, where HO_2^- approaches the steady-state concentration within 10–20 ms. From these results, the direct oxygen atom transfer shown by reaction 2 would seem to be most reasonable for initiation of the decomposition of ozone.

In Figure 8, superoxide ion and ozonide ion are formed in the reaction between ozone and HO_2^- in 0.117 M $[OH^-]$ solution as would be predicted from eq 4. However, it should be noted in the figure that O_2^- also accumulates after the consumption of ozone. This suggests an additional reaction (18) for the formation

$$O_3^- + OH \rightarrow 2O_2^- + H^+ \qquad (18)$$

of O_2^- from O_3^-, because O_3^- is the only species that remains in any appreciable concentration after the consumption of ozone. The role of the OH radical is supported by the experimental result that O_2^- is not generated by the decomposition of ozone if excess Na_2CO_3 (0.01 M) is present in the solution.

Under the conditions of the experiments reported here, the effect of the additional side-reactions proposed by Hart[18]

$$O_3^- + OH \rightarrow HO_2^- + O_2 \qquad (19)$$

$$O_3^- + OH \rightarrow O_3 + OH^- \qquad (20)$$

would be minimal. However, the final stages of ozone decomposition in highly basic solution such as is depicted in Figure 4 might provide additional evidence for reactions 19 and 20.

It is also interesting to note that the reaction of ozone with HO_2^- in the low-$[OH^-]$ solutions is slower in the initial stage than in the following latter stage (Figure 7). Again, the result may be explained by considering the rate of O_3^- decomposition, which proceeds in additional reactions with ozone. The value of $k_{HO_2^-} = 2.2 \times 10^6\ M^{-1}\ s^{-1}$ calculated from the initial rate of the accumulated trace shown in Figure 7 should reveal the true rate constant for reaction 4.

Consequently, the true rate constant for the initiation process for the decomposition of ozone can be determined from the kinetic experiments, which are carried out in the presence of Na_2CO_3 in low- and high-$[OH^-]$ solutions. On the basis of the reaction processes that are initiated by means of reaction 2 followed by reactions 4 and 5, the rate constant of reaction 2 corrected for the stoichiometry is $111/3 = 37\ M^{-1}\ s^{-1}$ or $130/3 = 43\ M^{-1}\ s^{-1}$, on the basis of the results shown in Figures 3 and 5, respectively.

In summary, a generalized empirical rate law can be written for the decomposition of aqueous solutions of ozone:

$$\text{rate} = k_{OH^-}[O_3][OH^-] + k_2[O_3]^2[OH^-] \qquad (21)$$

However, the values of k_{OH^-} and k_2 vary markedly with solution composition (i.e. ozone and OH^- concentration, the presence of absences of scavengers such as CO_3^{2-}, PO_4^{3-}, etc.). This generalized rate law (eq 21) is consistent with the following mechanistic steps:

initiation

$$O_3 + OH^- \rightarrow HO_2^- + O_2 \quad 40\ M^{-1}\ s^{-1}$$

propagation/termination

$$HO_2^- + O_3 \rightarrow O_3^- + HO_2 \quad 2.2 \times 10^6\ M^{-1}\ s^{-1}$$

$$HO_2 + OH^- \rightarrow O_2^- + H_2O \quad pK = 4.8$$

$$O_2^- + O_3 \rightarrow O_3^- + O_2 \quad 1.6 \times 10^9\ M^{-1}\ s^{-1}$$

$$O_3^- + H_2O \rightarrow OH + O_2 + OH^- \quad 20\text{–}30\ s^{-1}$$

$$O_3^- + OH \rightarrow O_2^- + HO_2 \quad 6 \times 10^9\ M^{-1}\ s^{-1}$$

$$O_3^- + OH \rightarrow O_3 + OH^- \quad 2.5 \times 10^9\ M^{-1}\ s^{-1}$$

$$OH + O_3 \rightarrow HO_2 + O_2 \quad 3 \times 10^9\ M^{-1}\ s^{-1}$$

$$OH + CO_3^{2-} \rightarrow OH^- + CO_3^- \quad 4.2 \times 10^8\ M^{-1}\ s^{-1}$$

$$CO_3^- + O_3 \rightarrow \text{products } (CO_2 + O_2^- + O_2)$$

$$HO_2^- + H_2O \rightleftharpoons H_2O_2 + OH^- \quad pK = 11.65$$

Additional steps that contribute minor pathways for the base-catalyzed decomposition of ozone have been described in detail by Hart, Hoigné, and co-workers.[15-19]

Acknowledgment. The authors express appreciation to the Japan Society for the Promotion of Science for a fellowship (G.G.).

Registry No. O_3, 10028-15-6; Na_2CO_3, 497-19-8.